



THE UNIVERSITY *of* EDINBURGH

Edinburgh Research Explorer

Prediction of intramuscular fat content and shear force in Texel lamb loins using combinations of different X-ray computed tomography (CT) scanning techniques

Citation for published version:

Clelland, N, Bungler, L, McLean, KA, Knott, S, Matthews, KR & Lambe, NR 2018, 'Prediction of intramuscular fat content and shear force in Texel lamb loins using combinations of different X-ray computed tomography (CT) scanning techniques', *Meat Science*, vol. 140, pp. 78-85.
<https://doi.org/10.1016/j.meatsci.2018.03.003>

Digital Object Identifier (DOI):

[10.1016/j.meatsci.2018.03.003](https://doi.org/10.1016/j.meatsci.2018.03.003)

Link:

[Link to publication record in Edinburgh Research Explorer](#)

Document Version:

Peer reviewed version

Published In:

Meat Science

Publisher Rights Statement:

© 2018 Elsevier Ltd. All rights reserved.

General rights

Copyright for the publications made accessible via the Edinburgh Research Explorer is retained by the author(s) and / or other copyright owners and it is a condition of accessing these publications that users recognise and abide by the legal requirements associated with these rights.

Take down policy

The University of Edinburgh has made every reasonable effort to ensure that Edinburgh Research Explorer content complies with UK legislation. If you believe that the public display of this file breaches copyright please contact openaccess@ed.ac.uk providing details, and we will remove access to the work immediately and investigate your claim.



1 **Prediction of intramuscular fat content and shear force in Texel lamb loins using**
2 **combinations of different x-ray computed tomography (CT) scanning techniques**

3
4 **N. Clelland^{1*}, L. Bunger¹, K.A. McLean¹, S. Knott², K. Matthews³ and N.R. Lambe¹**

5
6 *¹Animal Breeding and Genetics, Animal and Veterinary Sciences group, Scotland's Rural*
7 *College, West Mains Road, Edinburgh, EH9 3JG, United Kingdom*

8 *²Institute of Evolutionary Biology, School of Biological Sciences, University of Edinburgh,*
9 *Ashworth Laboratories, West Mains Road, Edinburgh, EH9 3JT, UK*

10 *³English beef and lamb executive, Agriculture and Horticulture Development Board,*
11 *Stoneleigh Park, Kenilworth, Warwickshire, CV8 2TL.*

12
13 *Address for correspondence:

14 Scotland's Rural College

15 Roslin Institute Building

16 Edinburgh

17 EH25 9RG

18 United Kingdom

19 Tel: +44131 651 9293

20 Email:Neil.Clelland@sruc.ac.uk

21

22

23

24

25

26 **Abstract**

27 Computed tomography (CT) parameters, including spiral computed tomography scanning
28 (SCTS) parameters, intramuscular fat (IMF) and mechanically measured shear force were
29 derived from two previously published studies. Purebred Texel (n = 377) of both sexes,
30 females (n = 206) and intact males (n = 171) were used to investigate the prediction of IMF
31 and shear force in the loin. Two and three dimensional CT density information was available.
32 Accuracies in the prediction of shear force and IMF ranged from R^2 0.02 to R^2 0.13 and R^2
33 0.51 to R^2 0.71 respectively, using combinations of SCTS and CT scan information. The
34 prediction of mechanical shear force could not be achieved at an acceptable level of accuracy
35 employing SCTS information. However, the prediction of IMF in the loin employing
36 information from SCTS and additional information from standard CT scans was successful,
37 providing evidence that the prediction of IMF and related meat eating quality (MEQ) traits
38 for Texel lambs *in vivo* can be achieved.

39

40 **Keywords:** spiral x-ray computed tomography, lamb, meat quality, intramuscular fat.

41

42 **1. Introduction**

43 Computed tomography (CT) is a non-invasive, diagnostic tool initially developed for use in
44 human medicine to improve the imaging of soft tissue structures and assist in diagnosing
45 conditions or diseases not directly associated with bone structure. Over the last few decades
46 CT has been adopted for use in animal breeding and is now routinely used in selective
47 breeding programs for sheep in the UK to accurately estimate carcass composition of live
48 animals. More recently, the prediction of aspects of meat quality (MQ) such as intramuscular
49 fat levels (IMF), fatty acid profiles and tissue composition have been investigated both *in*
50 *vivo* and post mortem in meat producing species (Font-i-Furnols, Brun, Tous, & Gispert,

51 2013; Kongsro & Gjerlaug-enger, 2013; L. Bünger, J.M. Macfarlane, N. R. Lambe, J.
52 Conington, K. A. McLean, K. Moore, 2011; Prieto et al., 2010). The basic principle of CT is
53 the measurement of the spatial distribution of any physical quantity. Offering greater contrast
54 in the imaging of soft tissue to that seen in conventional radiography (Kalender, 2006). The
55 first method of image capture most commonly used is ‘single-slice’ scanning. During single-
56 slice scanning, x-rays are used to generate cross-sectional, two-dimensional images of the
57 selected region of a subject. Each image is produced by rotation of the x-ray tube 360° around
58 the subject. Attenuation of radiation through the tissues can then be measured, with
59 differences indicating different tissue densities.

60

61 Advances in scanning technology have resulted in the development of contiguous scanning
62 procedures such as spiral CT scanning (SCTS), capable of producing a series of images in a
63 single contiguous scan at intervals of as little as 0.6 mm apart. The advantage is that multiple
64 images can be acquired faster, at reduced intervals, resulting in increased information
65 acquisitions in less time. Recent studies provide evidence that muscle density information
66 from single or multiple CT scans in sheep, can provide moderately accurate predictions of
67 IMF content *in vivo*. Prediction accuracies range from $R^2 = 0.33$ to 0.68 using several
68 approaches including various CT parameters (Clelland et al., 2014; Karamichou, Richardson,
69 Nute, McLean, & Bishop, 2006; Lambe et al., 2008; Lambe, McLean, et al., 2010; J. M.
70 Macfarlane, 2006). The aim of this study was to investigate any gains in the prediction of
71 IMF content and shear force in the loins of Texel sheep that may be achieved by utilizing the
72 wealth of information that relatively new SCTS techniques may provide.

73

74

75

76 **2. Materials and Methods**

77 *2.1. Experimental animals*

78 The CT parameters, including SCTS parameters, IMF and shear force in the loin were
79 derived from two previously-published studies. The first of these studies (Exp. 1), was
80 conducted over two years (2003 to 2004) and investigated the use of various *in vivo*
81 measurement techniques (ultrasonography, video image analysis and CT), to predict carcass
82 and meat quality in purebred Texel (n = 240) and Scottish Blackface (n = 233) lambs. The
83 full study and methods are detailed in Lambe et al. (2008). The second study (Exp. 2) was
84 conducted in 2009 and investigated the genotypic effects of the Texel muscling quantitative
85 trait loci (TMQTL) on carcass and meat quality in purebred Texel lambs (n = 137). Full
86 details are published in Lambe et al. (2010). The combination of these data from Exp. 1 and
87 Exp. 2 comprised data from pure-bred Texel lambs (n = 377) of both sexes, females (n = 206)
88 and intact males (n = 171). Lambs were reared to weaning as either singles (n = 184), twins
89 (n = 168) or artificially hand reared (n = 25). Mean age at CT was 132 d (SD 21.1, range 91-
90 202 d); with mean live weight 35.3kg (SD 4.9, range 20-49kg). Lambs were CT scanned pre-
91 slaughter using a Siemens Somatom Esprit scanner. All lambs were lightly sedated
92 (Rompun[®], Bayer animal health, Bayer plc., Newbury, UK) at a dose of 0.1-0.2mg xylazine
93 hydrochloride/kg body weight, then secured in a purpose-built cradle before being CT-
94 scanned.

95

96 *2.2. Single-slice and spiral x-ray CT measurements and image analysis*

97 A series of spiral CT images at intervals of 8mm were selected from the loin region of each
98 lamb. The first image was taken where the transverse process of the 7th lumbar vertebra
99 appears and the last image in the series where the transverse process of the 1st lumbar
100 vertebra is no longer visible (Fig.1a). Two-dimensional cross-sectional single-slice scans

101 were also used, taken at two defined anatomical positions, through the top of the leg at the
102 ischium bone (ISC), and through the chest at the 8th thoracic vertebra (TV8), details of the
103 images used and the location are presented in Fig. 1b.

104

105 **Insert Figure 1 Here**

106

107 This two dimensional method of scanning at these particular anatomical sites (including an
108 additional scan at the 5th lumbar vertebra, which was not used in this study), is currently used
109 in UK terminal sire breeding programs to provide accurate predictions of fat and muscle
110 weights in the carcass. This method, defined as ‘reference’ scanning (L. Bünger, J.M.
111 Macfarlane, N. R. Lambe, J. Conington, K. A. McLean, K. Moore, 2011), optimizes the
112 number of images required to be taken across the body of the sheep while maximizing the
113 accuracy of estimations for carcass traits. Images were produced with a resolution of 512 x
114 512 pixels with a 450mm field of view, producing images with a pixel size of 0.77mm² in
115 two dimensions. Spiral images were produced at the same resolution and field of view at
116 intervals of 8mm, producing images with a voxel size of 6.2mm³.

117 Automated analyses were performed on the images produced, to separate carcass from non-
118 carcass tissues (Glasbey & Young, 2002), and calculate the density of each pixel in
119 Hounsfield units (HU), the standard quantitative scale for describing radiodensity. In the final
120 segmented image each pixel was allocated to fat, muscle or bone using image thresholding
121 techniques (Mann, Young, Glasbey, & McLean, 2003). The thresholds in Hounsfield units
122 (HU) defined for the CT scanner (Siemens Somatom Esprit single slice) were Fat = -174 to -
123 12HU, Muscle = -10 to 92HU and Bone = 94HU and above, based on previous calibration
124 trials. Areas (mm²) and average densities (HU) of muscle and fat in each two dimensional
125 image were calculated, as well as standard deviations of the density values allocated to each

126 tissue. Combining all pixels allocated as either fat or muscle enabled the use of a novel
127 average ‘soft tissue density’ and standard deviation. The SCTS images were used to calculate
128 weighted average densities of muscle, fat and soft tissue (average tissue density, in each
129 individual scan image, weighted for tissue area in that image and averaged across all images
130 in the spiral scan series). Volumes of each tissue (mm^3) were also calculated. The resulting
131 SCTS parameters included; weighted muscle and fat densities and relating standard
132 deviations, weighted soft tissue densities and standard deviation, and calculated muscle and
133 fat volumes (mm^3). The CT parameters measured from the two dimensional reference scans
134 in the ISC and TV8 regions were muscle density, fat density and related standard deviations,
135 as well as the soft tissue densities and standard deviations of soft tissue densities. Muscle area
136 and fat area tissue measurements (mm^2) were also calculated for each of the reference scan
137 images. Total CT predicted carcass fat (PrCfat), as a measure of subcutaneous and
138 intermuscular fat in the entire carcass, was also predicted using a breed-specific prediction
139 equation developed from previous research (Macfarlane et al., 2006):

$$140 \text{PrCfat}(kg) = (-2236 + (LW \times 80.26) + (ISCFA \times 0.21) + (LV5FA \times 0.19) +$$
$$141 (TV8FA \times 0.221))/1000$$

142 Where PrCfat is the CT predicted weight of subcutaneous and intermuscular fat (kg), LW is
143 live weight at CT scanning, ISCFA is the area of pixels allocated as fat in the scan image
144 taken at the ischium (mm^2), LV5FA is the area of pixels allocated as fat in the scan image
145 taken at the 5th lumbar vertebra (mm^2) and TV8FA is the area of pixels allocated as fat in the
146 scan image taken at the 8th thoracic vertebra. Details, acronyms and descriptions of each CT
147 and MQ trait are presented in Table1.

148

149

150

151 2.3. Slaughter procedure and meat quality parameter measurements

152 The loin muscle (*M. longissimus lumborum*) was removed from the right side of each carcass
153 included in Exp. 1, vacuum-packed aged for 7 days, and frozen prior to meat quality analysis
154 at the University of Bristol. Carcasses included in Exp. 2 were subjected to high voltage
155 electrical stimulation (700 volts RMS for 45 seconds applied between the end of the
156 processing line and the chiller), chilled and aged for between 7-9 d and dissected, removing
157 the loin muscle (*M. longissimus lumborum*) from the right side of the carcass. In both Exp. 1
158 and 2, IMF content was measured in a cross-sectional slice taken from the cranial end of the
159 muscle at the first lumbar vertebra. Each sample was blended to a fine paste and IMF content
160 was measured using petroleum ether (B.P. 40-60°C) as the solvent in a modified Soxhlet
161 extraction (AOAC, 1990). Mean IMF was 1.48% (SD 0.68) and ranged from 0.27 – 3.88%.
162 The majority of lambs were slaughtered 4-8 d after CT scanning (n=217), and the remaining
163 lambs were slaughtered 32-33 d after CT scanning (n=160), to allow for a 30 day withdrawal
164 period from the CT sedative and subsequent taste panel analysis (which formed part of a
165 wider study). Shear force was also measured, using a TA-XT2 texture analyzer (Stable Micro
166 System, Surrey, UK) fitted with Volodkevich-type jaws, a standard compression method to
167 determine tenderness simulating the action of the incisor tooth (Volodkevich, 1938). Loins
168 were cooked ‘sous-vide’ (in vacuum pack bags) in a water bath at 80°C to an internal core
169 temperature of 78°C (Teye et al., 2006) monitoring individual loin temperature using a digital
170 temperature probe (Hanna Instruments UK, Eden Way, Bedfordshire) . Samples were then
171 immediately cooled in iced water and held at 4°C overnight for a minimum period of 12
172 hours. Ten 10 x 10 x 20mm samples were cut from each loin following the direction of the
173 muscle fibers and sheared at a constant speed of 1mm/s perpendicular to the muscle fiber
174 direction. Shear force was recorded as the force required (kgF) to compress the sample, with

175 greater values for less tender samples. Results were averaged over the ten samples taken from
176 each loin. Mean shear force was 3.4kgF (SD 1.56) and ranged from 1.39 – 10.72kgF.

177

178 *2.4. Statistical analysis*

179 Lambs with no IMF data were removed (n = 2), lambs without full CT information were
180 removed (n = 2), and finally lambs with IMF content greater than three standard deviations
181 from the mean were identified as outliers and also removed (n = 3). Initial regression analysis
182 and subsequent model checking (Distribution of residuals) suggested the need for
183 transformation of shear force data. As a result shear force was log-transformed and fitted to a
184 normal distribution prior to any regression analysis. The number of days from CT scanning to
185 slaughter (group 1: 4-8 d; group 2: 32-33 d, accounting for lambs subjected to a withdrawal
186 period to allow subsequent taste panel analysis) was tested using a general analysis of
187 variance in Genstat14TM adjusted for PrCfat, and provided evidence of no significant effect
188 on IMF content (P = 0.80) or shear force (P = 0.07). The term was also fitted as an
189 independent variable in the simple regression models in order to test the relationship between
190 days to slaughter and the CT parameters and was again not significant when tested on IMF (P
191 = 0.71) and shear force (P = 0.19) therefore was not included in the analysis. A summary of
192 the CT traits tested in the models are presented in Table 1. Histograms of MQ traits (shear
193 force prior to transformation and IMF) are presented in Fig. 2.

194

195

196

197

198

199

200 **Table 1:** Acronyms and summary statistics of both CT and meat quality traits along with trait
 201 descriptions, means and standard deviations (SD) in the Texel data utilized in the prediction
 202 of IMF (n = 370)

Trait	Acronym	Trait Description	Mean	SD
CT Traits				
	ISCMD	Average muscle density in 2D scan at the ischium (HU)	48.44	2.10
	ISCMSD	SD of muscle density in 2D scan at the ischium (HU)	16.81	0.81
	ISCFD	Average fat density in 2D scan at the ischium (HU)	-62.37	5.32
	ISCFSD	SD of fat density in 2D scan at the ischium (HU)	36.51	2.50
	ISCFA	Carcass fat area measured in 2D scan at the ischium (mm ²)	3651	1404
	ISCA	Muscle area measured in 2D scan at the ischium (mm ²)	27415	2898
	TV8MD	Average muscle density in 2D scan at the 8 th thoracic vertebra (HU)	44.68	2.98
	TV8MSD	SD of muscle density in 2D scan at the 8 th thoracic vertebra (HU)	21.94	1.73
	TV8FD	Average fat density in 2D scan at the 8 th thoracic vertebra (HU)	-64.64	5.99
	TV8FSD	SD of fat density in 2D scan at the 8 th thoracic vertebra (HU)	39.21	3.16
	TV8FA	Carcass fat area measured in 2D scan at the 8 th thoracic vertebra (mm ²)	3451	1843
	TV8MA	Muscle area measured in 2D scan at the 8 th thoracic vertebra (mm ²)	12380	1833
	ISCSTD	Average soft tissue density in 2D scan at the ischium (HU)	35.55	5.07
	ISCSTSD	SD of soft tissue density in 2D scan at the ischium (HU)	40.34	5.66
	TV8STD	Average soft tissue density in 2D scan at the 8 th thoracic vertebra (HU)	21.84	11.35
	TV8STSD	SD of soft tissue density in 2D scan at the 8 th thoracic vertebra (HU)	50.56	6.69
	w_md	Average muscle density in the loin spiral scan (weighted by area in each component image) (HU)	46.13	2.22
	w_ms	SD of muscle density in the loin spiral scan (weighted by area in each component image) (HU)	19.91	1.25
	w_fd	Average fat density in the loin spiral scan (weighted by area in each component image) (HU)	-63.97	4.65
	w_fsd	SD of fat density in the loin spiral scan (weighted by area in each component image) (HU)	40.63	3.49
	m_vol	Muscle tissue volume in the loin spiral scan (cm ³)	1827	281
	f_vol	Fat tissue volume in the loin spiral scan (cm ³)	298	180
	w_std	Soft tissue density in the loin spiral scan weighted by area (HU)	31.41	8.43
	w_stsd	SD of soft tissue in the loin spiral scan weighted by area (HU)	42.79	6.17
	PrCfat	Predicted total carcass fat weight (kg)	2.34	1.11
MQ Traits				
	Shear force	<i>M. longissimus lumborum</i> shear force (kgF)	3.40	1.56
	IMF	<i>M. longissimus lumborum</i> intra-muscular fat (%)	1.48	0.68

203

204

205 **Insert Figure 2 Here**

206

207 Sixteen models were tested in the analyses (Table 2), termed models A-P using information
208 from SCTS only (^{sp}) and a combination of SCTS and reference information (^{com}). Models
209 with one or two variables included in the maximum model were analyzed using simple and
210 multiple linear regression, respectively, whilst models employing CT data with more than
211 two variables were analyzed using stepwise linear regression in Genstat14TM (Payne, Murray,
212 Harding, Baird, & Soutar, 2011), to optimize the number and combination of independent
213 variables from the maximum fitted model. Models were then tested for significant differences
214 between correlation coefficients ($\sqrt{\text{Adj } R^2}$) applying standard methods using Fisher's Z
215 transformation (Mudholkar, 2006). Final models were identified as those with significantly
216 greater prediction accuracies of MQ traits than the baseline model (Model A). These models
217 were then validated. During validation, available data were split using a natural time series
218 separation in the data, as described by Snee (1977). Experiment one data was employed as a
219 calibration data set, and experiment two data as a validation data set. Summary statistics for
220 MQ traits and CT measured traits for both calibration and validation data sets are presented in
221 Table 3, Histograms of MQ traits (shear force prior to transformation and IMF) are presented
222 in Fig. 3.

223

224

225

226

227

228

229

230

231

232 **Table 2:** Terms included in the maximum linear regression models tested prior to stepwise
 233 regression using both spiral CT scan parameters only (sp) and spiral CT scan parameters
 234 alongside two-dimensional reference scan parameters (com). Explanations of acronyms used
 235 in the models can be found in Table 1

Maximum Models	
SCTS parameters only (sp)	SCTS + 2D reference scan parameters (com)
A PrCfat	PrCfat
B PrCfat, w_md	PrCfat, w_md, ISCMD, TV8MD
C PrCfat, w_fd	PrCfat, w_fd, ISCFD, TV8FD
D PrCfat, m_vol	PrCfat, m_vol, ISCMA, TV8MA
E PrCfat, f_vol	PrCfat, f_vol, ISCFA, TV8FA
F PrCfat, w_md, w_fd	PrCfat, w_md, w_fd, ISCMD, TV8MD
G PrCfat, m_vol, f_vol	PrCfat, m_vol, f_vol, ISCMA, TV8MA, ISCFA, TV8FA
H PrCfat, w_md, w_msd	PrCfat, w_md, w_msd, ISCMD, ISCMSD, TV8MD, TV8MSD
I PrCfat, w_fd, w_fsd	PrCfat, w_fd, w_fsd, ISCFD, ISCFSD, TV8FD, TV8FSD
J PrCfat, w_md, w_msd, w_fd, w_fsd	PrCfat, w_md, w_msd, w_fd, w_fsd, ISCMD, ISCMSD, TV8MD, TV8MSD, ISCFD, ISCFSD, TV8FD, TV8FSD
K PrCfat, w_md, w_msd, w_fd, w_fsd, f_vol	PrCfat, w_md, w_msd, w_fd, w_fsd, f_vol, ISCMD, ISCMSD, TV8MD, TV8MSD, ISCFD, ISCFSD, TV8FD, TV8FSD, ISCFA, TV8FA
L PrCfat, w_md, w_msd, w_fd, w_fsd, m_vol, f_vol	PrCfat, w_md, w_msd, w_fd, w_fsd, m_vol, f_vol, ISCMD, ISCMSD, TV8MD, TV8MSD, ISCFD, ISCFSD, TV8FD, TV8FSD, ISCMA, ISCFA, TV8MA, TV8FA
M PrCfat, w_std	PrCfat, w_std, ISCSTD, TV8STD
N PrCfat, w_std, w_stsd	PrCfat, w_std, w_stsd, ISCSTD, ISCSTSD, TV8STD, TV8STSD
O PrCfat, w_std, w_stsd, f_vol	PrCfat, w_std, w_stsd, f_vol, ISCSTD, ISCSTSD, TV8STD, TV8STSD, ISCFA, TV8FA
P PrCfat, w_std, w_stsd, f_vol, m_vol	Pr_Cfat, w_std, w_stsd, f_vol, m_vol, ISCSTD, ISCSTSD, TV8STD, TV8STSD, ISCFA, ISCMA, TV8FA, TV8MA

236

237 The fitted terms identified in the most accurate prediction models derived from the regression
 238 analyses using the entire data set were used to produce prediction equations using the
 239 calibration data set (Exp. 1). These equations were then used to predict MQ traits of the
 240 lambs included in the independent validation data set (Exp. 2). The coefficient of
 241 determination (R^2) and residual mean square error of prediction (RMSEP) were calculated for
 242 the predicted MQ traits against chemically extracted IMF and mechanical shear force, to
 243 identify the simplest and most reliable single predictive model or group of predictive models.

244

245 **Insert Figure 3 Here**

246

247 **Table 3:** Acronyms and summary statistics of both CT and meat quality traits, means and
248 standard deviations (SD) in the calibration and validation data sets: trait descriptions, means
249 and standard deviations (SD)

Trait	Acronym	Calibration Data (n=236)		Validation Data (n=134)	
		Mean	SD	Mean	SD
CT Traits					
	ISCMD	49.32	1.78	46.90	1.69
	ISCMSD	16.87	0.76	16.71	0.89
	ISCFD	-63.48	5.59	-60.43	4.14
	ISCFSD	35.89	1.97	37.57	2.97
	ISCFA	3999	1425	3060	1164
	ISMA	28328	2486	25823	2887
	TV8MD	44.89	2.98	44.24	2.97
	TV8MSD	21.52	1.68	22.69	1.56
	TV8FD	-64.66	6.58	-64.59	4.84
	TV8FSD	38.48	2.93	40.45	3.18
	TV8FA	3603	1990	3209	1541
	TV8MA	12859	1646	11533	1834
	ISCSTD	35.39	5.45	35.77	4.33
	ISCSTSD	41.77	5.88	37.88	4.23
	TV8STD	21.87	12.25	21.62	9.66
	TV8STSD	50.32	7.41	51.06	5.16
	PrCfat	2.60	1.08	1.88	1.01
	w_md	45.98	2.30	46.40	2.05
	w_msd	20.11	1.25	19.55	1.19
	w_fd	-64.36	4.41	-63.29	5.01
	w_fsd	40.37	3.46	41.08	3.52
	m_vol	1908	261	1686	259
	f_vol	329	195	244	133
	w_std	30.35	9.18	33.27	6.55
	w_stsd	43.65	6.57	41.27	5.09
MQ Traits					
	Shear force	3.73	1.69	2.82	1.08
	IMF	1.60	0.79	1.31	0.54

250

251

252 **3. Results**

253 *3.1. Predicting shear force and IMF content using SCTS information*

254 Very little of the variation in shear force was accounted for by PrCfat ($\text{Adj } R^2 = 0.05$),
255 however PrCfat accounted for a moderate amount of the variation in IMF ($\text{Adj } R^2 = 0.50$).
256 Compared to the baseline (Model A; Table 2), using only information from CT derived
257 predicted carcass fat, seven models that included additional CT variables, from the fifteen
258 models tested, were identified as being statistically significantly more accurate in the
259 prediction of IMF ($P > 0.05$). None of the additive models using only spiral CT information
260 were significantly more accurate ($P < 0.05$) in prediction of shear force when compared to the
261 baseline (Table 4).

262

263 From the seven models identified with significantly increased prediction ability of IMF when
264 compared to Model A, using only SCTS information, the model with the greatest accuracy
265 was identified as model L ($\text{Adj } R^2 = 0.70$). This model included CT predicted carcass fat
266 (PrCfat), weighted muscle density (w_md), fat volume and muscle volume (f_vol , m_vol),
267 resulting in the prediction equation:

268 " $y = 7.773 + 0.1808 \times PrCfat - 0.1379 \times w_md + 0.000000881 \times f_vol -$
269 $0.0000000338 \times m_vol$ "

270 The six remaining models including only SCTS information identified as better predictors of
271 IMF than PrCfat alone were compared with the maximum benchmark (Model L). Models
272 with significantly reduced accuracy ($P > 0.05$) compared to the benchmark model L were
273 discarded. This included model P (Table 4), which left a total of six models with correlation
274 coefficients that were not significantly different, essentially meaning that the prediction
275 ability of these six models is statistically similar, thus identifying a group of models that
276 would predict IMF equally using SCTS information. Model K was also dropped as it was

277 entirely the same final model as model J following stepwise linear regression. The final
278 selected models included; model B ($\text{Adj } R^2 = 0.67$), model F ($\text{Adj } R^2 = 0.68$), model H (Adj
279 $R^2 = 0.67$), model J ($\text{Adj } R^2 = 0.69$) and model L ($\text{Adj } R^2 = 0.70$).

280

281 *3.2. Predicting shear force and IMF content using a combination of SCTS and reference scan* 282 *information*

283 Models using both SCTS information (^{sp}) and a combination of SCTS information and
284 reference information (^{com}) were again compared to the simple linear model using only PrCfat
285 for the predictions of both shear force and IMF. In the analysis for the prediction of shear
286 force, prediction accuracies were significantly improved with the inclusion of information
287 from the reference scan images (ISC, TV8). Nonetheless, the overall results show that the
288 maximum prediction accuracy achieved for shear force, from models developed was $\text{Adj } R^2 =$
289 0.13 (Table 4).

290

291 In the prediction of IMF ten of the fifteen models tested were significantly greater in
292 prediction accuracies than that of PrCfat alone ($P < 0.05$). From these models the single ‘best’
293 model was identified as model L^{com} ($\text{Adj } R^2 = 0.71$) and used as a maximum benchmark
294 model:

$$295 \text{ "y} = 7.675 + 0.3125 * PrCfat - 0.0978 \times w_md + 0.0000000299 \times m_vol +$$
$$296 0.000001196 \times f_vol + 0.0168 \times ISCMD + 0.0371 \times ISCMSD - 0.0000393 \times ISCMA -$$
$$297 0.0543 \times TV8MD + 0.0000236 \times TV8MA - 0.0001298 \times TV8FA"$$

298 Where PrCfat is CT predicted carcass fat, w_md is weighted muscle density in the spiral
299 information, m_vol is the volume of muscle estimated from the spiral information, f_vol is
300 the volume of fat estimated from spiral information, ISCMD is the average muscle density in
301 the ischium scan region, ISCMSD is the standard deviation of muscle density in the ischium

302 scan region, ISCMA is the estimated area of muscle in the ischium scan region, TV8MD is
 303 the average density of muscle within the 8th thoracic vertebra region, TV8MA is the
 304 estimated muscle area within the 8th thoracic vertebra region and TV8FA is the estimated fat
 305 area within the 8th thoracic vertebra region.

306 All models were then tested against the benchmark and any that were statistically
 307 significantly different in prediction accuracy were discarded ($P > 0.05$), which included
 308 Model M^{com} (Adj R² = 0.63). These analyses therefore identified nine “best” models with
 309 similar prediction abilities: L^{com} (benchmark; Adj R² = 0.71); F^{com}, J^{com} and K^{com} (Adj R² =
 310 0.70); B^{com} and H^{com} (Adj R² = 0.68); O^{com} and P^{com} (Adj R² = 0.67); and N^{com} (Adj R² =
 311 0.66). Regression results for all models are presented in Table 4.

312 **Table 4:** Regression results for the prediction of ShF or IMF, presented is the adjusted
 313 coefficient of determination (Adj R²) and residual mean square error (RMSE) using
 314 information from SCTS only (sp) or a combination of SCTS and two-dimensional reference
 315 scans (com), using the whole dataset (n=370).

Model	ShF				IMF			
	sp		com		sp		com	
	Adj R ²	RMSE	Adj R ²	RMSE	Adj R ²	RMSE	Adj R ²	RMSE
A	0.03	0.16	0.03	0.16	0.51	0.48	0.50	0.47
B	0.03	0.16	0.07	0.16	0.67**	0.39	0.68**	0.39
C	0.04	0.16	0.05	0.16	0.51	0.48	0.52	0.48
D	0.04	0.16	0.04	0.16	0.56	0.46	0.60	0.43
E	0.03	0.16	0.10*	0.16	0.55	0.46	0.58	0.45
F	0.04	0.16	0.09	0.16	0.68**	0.39	0.70**	0.38
G	0.04	0.16	0.10*	0.16	0.58	0.45	0.60	0.43
H	0.04	0.16	0.09	0.16	0.67**	0.39	0.68**	0.39
I	0.05	0.16	0.09	0.16	0.55	0.46	0.56	0.46
J	0.05	0.16	0.12*	0.16	0.69**	0.38	0.70**	0.37
K	0.05	0.16	0.13*	0.15	0.69**	0.38	0.70**	0.37
L	0.06	0.16	0.13*	0.15	0.70**	0.38	0.71**	0.37
M	0.02	0.16	0.08	0.16	0.54	0.47	0.63*	0.42
N	0.02	0.16	0.09	0.16	0.57	0.45	0.66**	0.40
O	0.03	0.16	0.10*	0.16	0.59	0.44	0.67**	0.40
P	0.04	0.16	0.10*	0.16	0.62*	0.42	0.67**	0.39

316 ^{sp} Using SCTS information

317 ^{com} Using a combination of SCTS and reference CT information

318 * Adj R² differs significantly from the baseline model (A) ($P > 0.05$)

319 ** Adj R² does not differ significantly from the maximum benchmark model ($P < 0.05$)

320 *3.3. Model Validation and selection*

321 Given the poor prediction abilities of CT for shear force ($R^2 < 0.30$) using the parameters
322 tested, validation analysis for the prediction of shear force was not carried out. Fourteen
323 possible models in the prediction of IMF were identified. None of these models had
324 significantly less prediction accuracy ($P < 0.05$) than the single ‘best’ model from both SCTS
325 information and a combination of SCTS information and reference information (Model L^{com}),
326 so all were retained for validation analyses, with Adj R^2 ranging from 0.67 to 0.71. For
327 validation, fourteen prediction equations were derived using the calibration data set ($n = 236$),
328 corresponding to the independent variables identified in the final selected models from the
329 primary stepwise regression analysis. The models were then used to predict the chemical IMF
330 values of lambs included in the independent validation data set ($n = 134$). Final validation
331 results, coefficients of determination (R^2) and residual mean square errors of prediction
332 (RMSEP) are presented in Table 5.

333

334

335

336

337

338

339

340

341

342

343

344

345 **Table5:** Validation results: adjusted coefficient of determination ($\text{Adj } R^2$), residual mean
 346 square error (RMSE) of calibration; and coefficient of determination (R^2) and residual mean
 347 square error of prediction (RMSEP) of the validation data

Model	Calibration (n=236)		Validation (n=134)	
	Adj R^2	RMSE	R^2	RMSEP
B ^{sp}	0.69	0.41	0.60	0.34
F ^{sp}	0.70	0.41	0.59	0.34
H ^{sp}	0.69	0.41	0.60	0.34
J ^{sp}	0.70	0.41	0.62	0.33
L ^{sp}	0.71	0.40	0.62	0.33
B ^{com}	0.71	0.40	0.64	0.32
F ^{com}	0.71	0.40	0.64	0.32
H ^{com}	0.70	0.40	0.64	0.32
J ^{com}	0.72	0.40	0.66	0.31
K ^{com}	0.71	0.40	0.65	0.32
L ^{com}	0.72	0.39	0.65	0.32
N ^{com}	0.66	0.43	0.67	0.31
O ^{com}	0.67	0.43	0.64	0.32
P ^{com}	0.67	0.42	0.64	0.32

348 ^{sp} Model uses information from spiral scans only

349 ^{com} Model uses information from a combination of spiral and two dimensional scans

350

351 The model with the strongest validity was model N^{com} ($R^2 = 0.67$, RMSEP = 0.31)

352 using both SCTS information and reference scan information, including CT predicted carcass

353 fat (PrCfat), weighted density of soft tissue and its standard deviation (w_std and w_stsd) in

354 the spiral scan of the loin, soft tissue density and its standard deviation in the ischium scan

355 (ISCSTD and ISCSTSD), soft tissue density in the 8th thoracic vertebra scan and its standard

356 deviation (TV8STD and TV8STSD). This model (N^{com}, $R^2 = 0.67$) was then used as a

357 maximum benchmark and the thirteen remaining models also included in the validation

358 analysis were tested against the maximum benchmark using Fisher's z transformation (Rasch

359 et al., 1978). All of the models performed as well as the maximum benchmark model in the

360 validation analysis ($P < 0.05$; $R^2 = 0.59$ to 0.66). This left fourteen models for consideration

361 as predictors of IMF, five of which used SCTS information and nine which used a

362 combination of SCTS information and reference information. Details of the final selected

363 prediction models developed from the entire data set are presented in Table 6. These included
364 Models B^{SP}, F^{SP}, H^{SP}, J^{SP} and L^{SP} using SCTS information and models B^{com}, F^{com}, H^{com}, J^{com},
365 K^{com}, L^{com}, N^{com}, O^{com} and P^{com} using a combination of information from both the reference
366 scans and SCTS.

367
368 **Table 6:** Final prediction models and equations derived from the whole data set, adjusted
369 coefficient of determination (Adj R²) and residual mean square error of the prediction
370 (RMSEP)

Model	Final prediction model equation	Adj R ²	RMSEP
B ^{SP}	y=8.048+0.2508*PrCfat-0.1551*w_md	0.67	0.39
F ^{SP}	y=7.897+0.2347*PrCfat-0.1720*w_md-0.01514*w_fd	0.68	0.39
H ^{SP}	y=7.10+0.2326*PrCfat-0.1474*w_md+0.0319*w_msd	0.67	0.39
J ^{SP}	y=7.62+0.1134*Pr_Cfat-0.1566*w_md+0.0401*w_msd-0.02682*w_fd-0.0417*w_fsd	0.69	0.38
L ^{SP}	y=7.773+0.1808*PrCfat-0.1379*w_md+0.000000881*f_vol-0.000000038*m_vol	0.70	0.38
B ^{com}	y=8.275+0.2248*PrCfat-0.1113*w_md-0.0490*TV8MD	0.68	0.39
F ^{com}	y=7.794+0.1704*PrCfat-0.1347*w_md-0.01553*w_fd+0.0183*ISCMD-0.0600*TV8MD-0.00471*TV8FD	0.70	0.38
H ^{com}	y=7.39+0.2079*PrCfat-0.1043*w_md+0.0298*w_msd-0.0488*TV8MD	0.68	0.39
J ^{com}	y=6.66+0.1054*PrCfat-0.1138*w_md+0.0661*w_msd-0.02761*w_fd-0.0250*w_fsd-0.0502*TV8MD	0.70	0.37
K ^{com}	y=5.78-0.1051*w_md+0.0549*w_msd-0.01753*w_fd+0.000000769*f_vol+0.0437*ISCMSD- 0.00703*ISCFD-0.0189*ISCFSD-0.0533*TV8MD	0.70	0.37
L ^{com}	y=7.675+0.3125*PrCfat-0.0978*w_md- 0.000000299*m_vol+0.000001196*f_vol+0.0168*ISCMD+0.0371*ISCMSD-0.0000393*ISCMA- 0.0543*TV8MD+0.0000236*TV8MA-0.0001298*TV8FA	0.71	0.37
N ^{com}	y=7.099+0.1101*PrCfat-0.0305*w_std-0.0368*w_std-0.0205*ISCSTD- 0.04523*TV8STD+0.0103*ISCSTSD-0.0404*TV8STSD	0.66	0.40
O ^{com}	y=7.382+0.2253*PrCfat-0.0251*w_std-0.0332*w_std+0.000001035*f_vol- 0.0322*ISCSTD+0.0142*ISCSTSD-0.04967*TV8STD-0.0387*TV8STSD-0.0001178*ISCFA- 0.0001394*TV8FA	0.67	0.40
P ^{com}	y=8.554+0.4879*PrCfat-0.0330*w_std-0.0448*w_std+0.000001051*f_vol-0.000000243*m_vol- 0.0000566*ISCMA-0.05713*TV8STD-0.0357*TV8STSD-0.0002859*TV8FA+0.0000371*TV8MA	0.67	0.39

371 ^{SP} Model uses information from spiral scans only

372 ^{com} Model uses information from a combination of spiral and two dimensional scans

373

374 4. Discussion

375 It has been demonstrated in previous studies that information from single or multiple CT
376 scans can provide moderately accurate predictions of IMF in different sheep breeds.

377 Prediction accuracies range from R² = 0.33 to 0.68. (Clelland et al., 2014; Karamichou,

378 Richardson, Nute, McLean, & Bishop, 2006; Lambe, McLean, et al., 2010; J. Macfarlane,
379 Lewis, Emmans, Young, & Simm, 2006) These studies have provided evidence of the
380 potential use of single-slice CT scanning as a predictor of IMF in different sheep breeds.

381 The results from this study provide evidence that further improvements in the prediction of
382 IMF are possible and the use of information from both spiral CT scans and a combination of
383 spiral CT scans and reference scans can adequately predict intramuscular fat content in the
384 loin of purebred Texel sheep.

385

386 Prediction models using CT parameters in the assessment of IMF content, achieved a
387 maximum accuracy of $\text{AdjR}^2 = 0.70$ and 0.71 , using either spiral information only, or a
388 combination of spiral and reference scan information respectively. The results from this study
389 indicate that there are several potential prediction models that may be developed, using
390 different combinations of CT parameters. There was a group of potential prediction models
391 with increasing degrees of complexity that had similar prediction accuracies for IMF, which
392 could be indicative of a possible ‘ceiling’ in the achievable prediction accuracies we may
393 expect using these types of CT parameters. Models that included increasing numbers of
394 independent variables appeared to be slightly less transferable when validated against the
395 independent time series data. Although not significant, the models including fewer
396 independent variables and more direct measures of soft tissue density (average and standard
397 deviation) were generally more robust during validation. This suggests that the complexity of
398 the model may have an effect on the accuracy of prediction when applied to an independent
399 data set.

400

401 Given that there are few, if indeed any, *in vivo* predictors of MQ traits in meat producing
402 species, prediction accuracies may be acceptable with a suggested lower limit of $\text{R}^2 = 0.30$.

403 However in this study the use of CT parameters failed to adequately estimate shear force of
404 the loin producing an upper limit of $R^2 = 0.13$. Similar studies carried out by Lambe et al.
405 (2008) and Karamichou et al. (2006) reported low phenotypic correlations between two
406 dimensional CT parameters and shear force ($r = 0.15 - 0.22$, $r = 0.16$ respectively). Although
407 IMF is regarded as an important factor in the eating quality of meat when related to mouth
408 feel, tenderness, juiciness and species-specific flavor, the relationship between shear force
409 and IMF is less clear. Other factors such as cooking loss, ultimate pH, post-mortem
410 glycolysis and conditioning (ageing) play an important role in the conversion of muscle to
411 meat and may have significant effects on shear force results. The CT parameters of the same
412 muscle *in vivo* to that of a processed, aged and cooked piece of meat may be too far removed
413 for shear force parameter estimation or prediction to be possible. There is evidence of a linear
414 relationship between shear force values in cooked meat samples and solvent-extracted IMF
415 content in raw meat samples and it is generally accepted that this relationship exists
416 (Hopkins, Hegarty, Walker, & Pethick, 2006; Pannier et al., 2014; Safari, Fogarty, Ferrier,
417 Hopkins, & Gilmour, 2001), although the size of the effect is often debated.

418 Breeding programs in the UK for several species of livestock have resulted in substantial
419 genetic improvement in areas such as production efficiency. Genetic improvement in such
420 traits are permanent and cumulative (Simm, 1998). CT predictions of carcass fat and muscle
421 weights and muscularity in both the gigot and loin have been used in pedigree UK sheep
422 breeding programmes over the last two decades (L. Bünger, J.M. Macfarlane, N. R. Lambe, J.
423 Conington, K. A. McLean, K. Moore, 2011). Together with ultrasound measures of fat and
424 muscle depth in the loin region, CT measured carcass fat and muscle weights have
425 contributed much to the success of breeding for leaner carcasses (Moore, McLean, & Bunger,
426 2011). However, it remains that the drive for reduced carcass fatness and increased
427 muscularity in current breeding programmes is having an impact on IMF content and as a

428 result meat eating quality traits (Pannier et al., 2014). This study shows that there may be
429 several approaches using SCTS technology to predict IMF as a MQ trait and a proxy for meat
430 eating quality traits.

431

432 In conclusion, the prediction of mechanical shear force could not be achieved at an
433 acceptable level of accuracy employing information from SCTS information, or a
434 combination of reference scan image information and SCTS information. However, the
435 prediction of IMF in the loin employing information from SCTS with or without additional
436 information from reference scans was more promising. This study provides valuable evidence
437 that the prediction of IMF and related meat eating quality traits for Texel lambs *in vivo* can be
438 achieved using spiral x-ray CT technology. However the increase in accuracy when
439 employing SCTS technology was not significant when compared to previous studies using
440 single slice scanning procedures ($P < 0.05$; Clelland et al., 2014). This suggests that the use
441 of SCTS technology in the prediction of IMF does not adequately increase prediction
442 accuracies to justify additional image analysis involved in the processing of the resulting
443 data. Therefore the authors conclude that although the methods used in this study were
444 successful in the prediction of IMF, the increased image analysis and processing currently
445 required does not justify the increase in accuracy achieved when compared to current
446 reference scan procedures.

447

448 **Acknowledgements**

449 Funding for this work was gratefully received from AHDB Beef and Lamb, Quality meat
450 Scotland and HCC as part of Neil Clelland's PhD studies. Thanks go to Ian Richardson and
451 colleagues at the University of Bristol for performing laboratory tests as part of the historical
452 trials.

453 **References**

- 454 AOAC. (1990). *Official Methods of Analysis* (15th ed.). Association of Official Analytical
455 Chemists.
- 456 Clelland, N., Bunger, L., McLean, K. A., Conington, J., Maltin, C., Knott, S., & Lambe, N.
457 R. (2014). Prediction of intramuscular fat levels in Texel lamb loins using X-ray
458 computed tomography scanning. *Meat Science*, 98(2), 1–9.
459 <https://doi.org/10.1016/j.meatsci.2014.06.004>
- 460 Font-i-Furnols, M., Brun, A., Tous, N., & Gispert, M. (2013). Use of linear regression and
461 partial least square regression to predict intramuscular fat of pig loin computed
462 tomography images. *Chemometrics and Intelligent Laboratory Systems*, 122, 58–64.
463 <https://doi.org/10.1016/j.chemolab.2013.01.005>
- 464 Glasbey, C., & Young, M. J. (2002). Maximum a posteriori estimation of image boundaries
465 by dynamic programming. *Applied Statistics*, 51(2), 209–221.
- 466 Hopkins, D. L., Hegarty, R. S., Walker, P. J., & Pethick, D. W. (2006). Relationship between
467 animal age, intramuscular fat, cooking loss, pH, shear force and eating quality of aged
468 meat from sheep. *Australian Journal of Experimental Agriculture*, 46(6–7), 879–884.
469 <https://doi.org/10.1071/EA05311>
- 470 Kalender, W. A. (2006). X-ray computed tomography. *Physics in Medicine and Biology*,
471 51(13), R29–R43. <https://doi.org/10.1088/0031-9155/51/13/R03>
- 472 Karamichou, E., Richardson, R. I., Nute, G. R., McLean, K. a., & Bishop, S. C. (2006).
473 Genetic analyses of carcass composition, as assessed by X-ray computer tomography,
474 and meat quality traits in Scottish Blackface sheep. *Animal Science*, 82(2006), 151–162.
475 <https://doi.org/10.1079/ASC200518>
- 476 Kongsro, J., & Gjerlaug-enger, E. (2013). In vivo prediction of intramuscular fat in pigs using
477 computed tomography. *Journal of Animal Science*, 3(4), 321–325.
- 478 L. Bünger, J.M. Macfarlane, N. R. Lambe, J. Conington, K. A. McLean, K. Moore, C. A. G.
479 and G. S. (2011). Use of X-Ray Computed Tomography (CT) in UK Sheep Production
480 and Breeding. *CT Scanning-Techniques and Applications, INTECH ...*, 329–348.
481 Retrieved from [http://www.intechopen.com/books/ct-scanning-techniques-and-
482 applications/use-of-x-ray-computed-tomography-ct-in-uk-sheep-production-and-
483 breeding%5Cnhttp://www.intechopen.com/source/pdfs/20942/InTech-
484 Use_of_x_ray_computed_tomography_ct_in_uk_sheep_production_](http://www.intechopen.com/books/ct-scanning-techniques-and-applications/use-of-x-ray-computed-tomography-ct-in-uk-sheep-production-and-breeding%5Cnhttp://www.intechopen.com/source/pdfs/20942/InTech-Use_of_x_ray_computed_tomography_ct_in_uk_sheep_production_)
- 485 Lambe, N. R., Macfarlane, J. M., Richardson, R. I., Matika, O., Haresign, W., & Bunger, L.

486 (2010). The effect of the Texel muscling QTL (TM-QTL) on meat quality traits in
487 crossbred lambs. *Meat Science*, 85(4), 684–690.
488 <https://doi.org/10.1016/j.meatsci.2010.03.025>

489 Lambe, N. R., McLean, K. A., Macfarlane, J. M., Johnson, P. L., Jopson, N. B., Haresign,
490 W., ... Bunger, L. (2010). Predicting intramuscular fat content of lamb loin fillets using
491 CT scanning. In *Proceedings of the Farm Animal Imaging Congress Rennes* (pp. 9–10).

492 Lambe, N. R., Navajas, E. A., Schofield, C. P., Fisher, A. V., Simm, G., Roehe, R., &
493 Bünge, L. (2008). The use of various live animal measurements to predict carcass and
494 meat quality in two divergent lamb breeds. *Meat Science*, 80(4), 1138–1149.
495 <https://doi.org/10.1016/j.meatsci.2008.05.026>

496 Macfarlane, J., Lewis, R., Emmans, G., Young, M., & Simm, G. (2006). Predicting carcass
497 composition of terminal sire sheep using X-ray computed tomography. *Journal of*
498 *Animal Science*, 82(3), 289. <https://doi.org/10.1079/ASC200647>

499 Macfarlane, J. M. (2006). Growth, development and carcass quality in meat sheep and the use
500 of CT scanning as a tool for selection.

501 Mann, A. D., Young, M. J., Glasbey, C. A., & McLean, K. A. (2003). STAR: Sheep
502 Tomogram Analysis Routines. BioSS.

503 Moore, K., McLean, K. A., & Bunger, L. (2011). The benefits of computed tomography (CT)
504 scanning in UK sheep flocks for improving carcass composition. In *The British Society*
505 *of Animal Science and The Association of Veterinary Teaching and Research*.

506 Mudholkar, G. S. (2006). Fisher's Z-Transformation. In *Encyclopedia of Statistical Sciences*.
507 John Wiley & Sons, Inc. <https://doi.org/10.1002/0471667196.ess0796.pub2>

508 Pannier, L., Pethick, D. W., Geesink, G. H., Ball, A. J., Jacob, R. H., & Gardner, G. E.
509 (2014). Intramuscular fat in the longissimus muscle is reduced in lambs from sires
510 selected for leanness. *Meat Science*, 96(2), 1068–1075.
511 <https://doi.org/10.1016/j.meatsci.2013.06.014>

512 Payne, R., Murray, D., Harding, S., Baird, D., & Soutar, D. (2011). *Introduction to GenStat R*
513 *for Windows 14th Edition*. VSN International.

514 Prieto, N., Navajas, E. A., Richardson, R. I., Ross, D. W., Hyslop, J. J., Simm, G., & Roehe,
515 R. (2010). Predicting beef cuts composition, fatty acids and meat quality characteristics
516 by spiral computed tomography. *Meat Science*, 86(3), 770–779.
517 <https://doi.org/10.1016/j.meatsci.2010.06.020>

518 Safari, E., Fogarty, N. M., Ferrier, G. R., Hopkins, L. D., & Gilmour, A. (2001). Diverse
519 lamb genotypes. 3. Eating quality and the relationship between its objective

520 measurement and sensory assessment. *Meat Science*, 57(2), 153–159.
521 [https://doi.org/10.1016/S0309-1740\(00\)00087-5](https://doi.org/10.1016/S0309-1740(00)00087-5)

522 Simm, G. (1998). *Genetic improvement of cattle and sheep*. Ipswich: Farming Press.

523 Snee, R. D. (1977). Validation of Regression Models: Methods and Examples.
524 *Technometrics*, 19(4), 415–428. <https://doi.org/10.2307/1267881>

525 Teye, G. A., Sheard, P. R., Whittington, F. M., Nute, G. R., Stewart, A., & Wood, J. D.
526 (2006). Influence of dietary oils and protein level on pork quality. 1. Effects on muscle
527 fatty acid composition, carcass, meat and eating quality. *Meat Science*, 73(1), 157–165.
528 <https://doi.org/10.1016/j.meatsci.2005.11.010>

529 Volodkevich, N. N. (1938). Apparatus for measurements of chewing resistance or tenderness
530 of foodstuffs. *Journal of Food Science*, 3(1–2), 221–225. [https://doi.org/10.1111/j.1365-](https://doi.org/10.1111/j.1365-2621.1938.tb17056.x)
531 [2621.1938.tb17056.x](https://doi.org/10.1111/j.1365-2621.1938.tb17056.x)

532

533

534

535

Figure 1: Detailed tomogram's, single slice and spiral images produced during CT scanning
(a) First image where TPLV7 appears (i), last image where TPLV1 is no longer visible (ii) and 3D rendered stack of selected images (iii)
(b) Scan image from ischium region (i) and scan image from 8th thoracic vertebra region (ii)

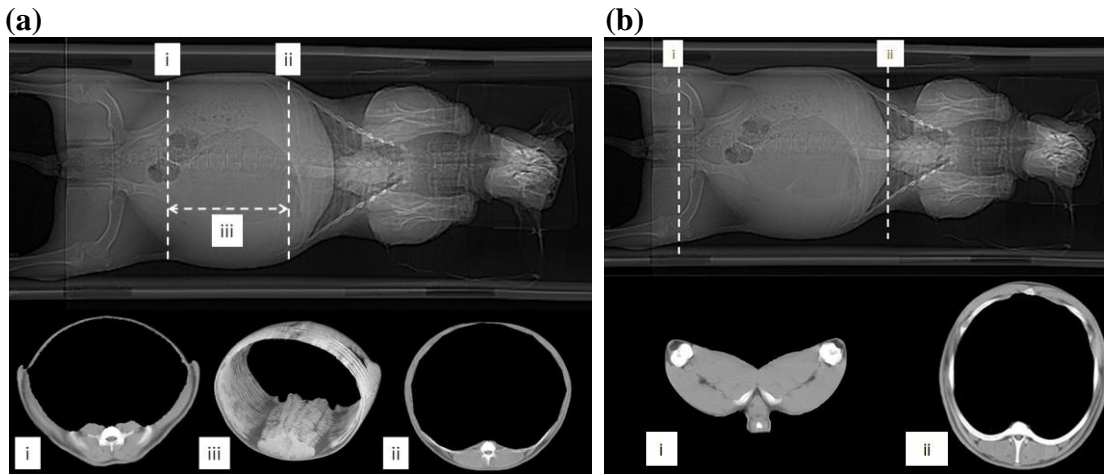


Figure 2: Histograms of chemically extracted intramuscular fat percentage (IMF %) and shear force (kgF) measured in the loin of the Texel lambs (n = 370)

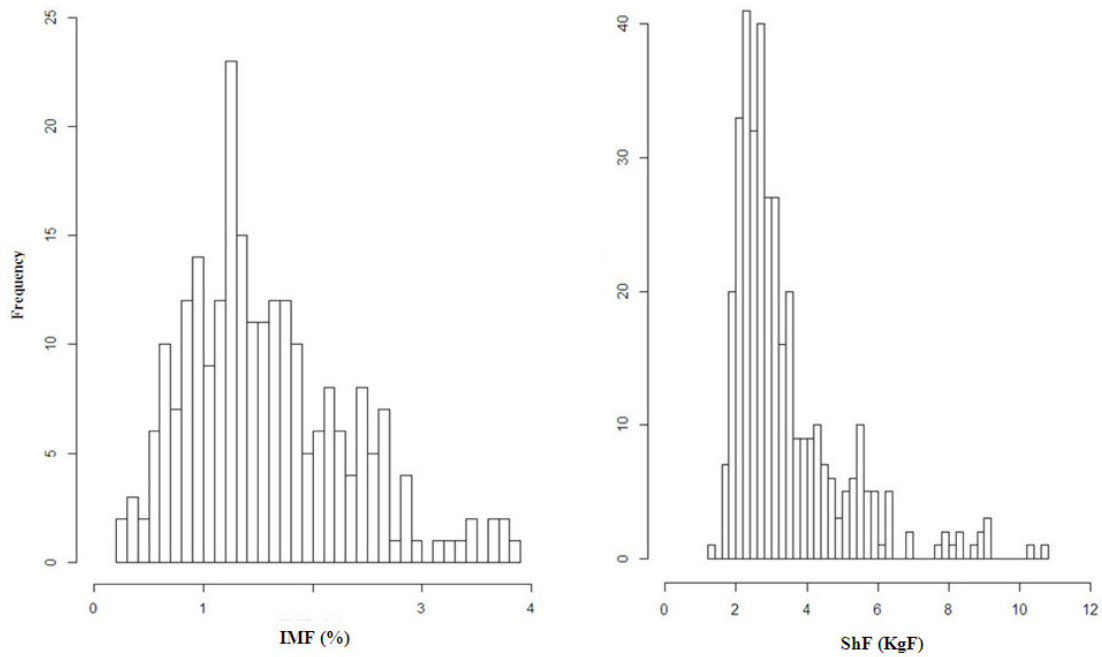
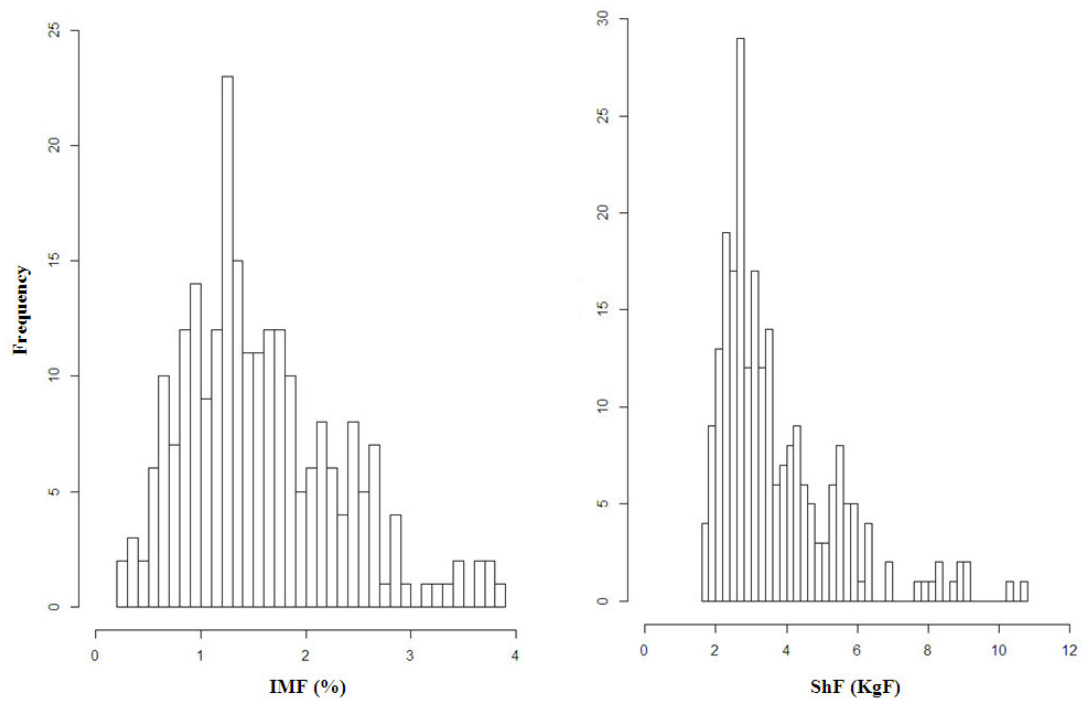


Figure 3: Histogram of chemically extracted intramuscular fat percentage (IMF %) and shear force (kgF) both measured in the loin in the calibration and validation data sets

Calibration (n=236)



Validation (n=134)

